

A fast, preparation-free method to detect iron in silicon

G. Zoth and W. Bergholz

Siemens AG, Components Group, Semiconductor Division, Otto-Hahn-Ring 6, 8000 Munich 83,
Federal Republic of Germany

(Received 13 October 1989; accepted for publication 10 February 1990)

Iron is one of the most important impurities in silicon integrated-circuit technology. We present a fast (5 min), essentially preparation-free large-area (25 cm^2) technique to determine the Fe concentration in boron-doped silicon with a sensitivity of $2\text{--}5 \times 10^{11}\text{ cm}^{-3}$. The principle of the method is based on the fact that interstitially dissolved Fe undergoes a reversible pairing reaction with boron and that the minority-carrier diffusion length—as measured by the surface photovoltage method—is modified by this reaction. The method has been calibrated by deep-level transient spectroscopy and is also suitable to measure a surface Fe contamination in combination with a rapid thermal annealing diffusion step.

I. INTRODUCTION

It is well established that in Si integrated-circuit technology contamination by fast-diffusing metal impurities like Fe, Ni, Cu, Cr, etc., can be a major yield-limiting factor.^{1,2} Highly integrated circuits of the ultra-large-scale integration (ULSI) era are even more susceptible to metal contamination than their large scale integration (LSI) and very-large-scale integration (VLSI) predecessors due to smaller device geometries, shallower junctions, and larger chip areas.³ Therefore, a comprehensive control and regular monitoring of contamination levels is an important prerequisite for obtaining high and stable device yields and good device reliabilities.

It is a general practical experience that iron is one of the most important impurities since it is a main constituent of many technically important materials and a common impurity in chemicals. Surface contamination levels of $5 \times 10^{12}\text{ cm}^{-2}$ have been shown to impair gate oxide integrity,⁴ and for bulk concentrations above 10^{15} cm^{-3} the formation of FeSi_2 rods has been found to be responsible for shorting $p\text{--}n$ junctions.^{5–7} From these findings and the anticipated increased sensitivity of advanced integrated circuits to contamination, a rule of thumb can be derived for the maximum permissible Fe contamination: An Fe concentration of 10^{13} cm^{-3} is probably critical, whereas 10^{12} cm^{-3} should be still safe.

The detection of iron in Si at a level of 10^{12} cm^{-3} or less is not possible by ion-beam techniques like secondary-ion-mass spectroscopy (SIMS), Rutherford backscattering (RBS), etc., but only by electrical [e.g., Hall effect or deep-level transient spectroscopy (DLTS)] or spectroscopic techniques like electron paramagnetic resonance (EPR).⁸ It is a common drawback of the latter techniques that they are quite time consuming and only sample small specimen volumes (typically $10^4\text{ }\mu\text{m}^3$ to 1 cm^3); i.e., they are far from ideal of large-scale monitoring purposes.

A fast large-area method to test for contamination by Fe, Ni, Cu, Co, and Pd is the so-called haze test.⁹ In this technique, the tendency of these elements to form a large density of near-surface precipitates is utilized for whole wafer detection. The disadvantages of this method are that it is

neither possible to derive an impurity concentration nor to distinguish between different elements. Furthermore, Fe detection by this method is often not reliable.¹⁰

A frequently employed method to obtain an overall measure of electrically active defects is to measure the minority-carrier lifetime or the minority-carrier diffusion length.¹¹ Although such measurements are comparatively simple and fast, a quantification or identification of an impurity is generally not possible.

As previously shown¹² the surface photovoltage (SPV) method for measuring the minority-carrier diffusion length L allows a separation of the contribution of Fe to the diffusion length in the important case of B-doped silicon. It is the purpose of this paper to demonstrate that the SPV method can be used as a fast (5 min), practically preparation-free large-area (25 cm^2) detection method for Fe in B-doped Si with a sensitivity of about $2 \times 10^{11}\text{ cm}^{-3}$ and that it can be applied to screen a large number of wafers for Fe contamination.

II. EXPERIMENTAL DETAILS

The SPV method¹³ is a standard method for the measurement of the minority-carrier diffusion length in semiconductors; it is described in detail by ASTM report F391.¹⁴ In this method, the sample is illuminated with monochromatic light of different wavelengths and therefore different penetration depths α^{-1} (α is the absorption coefficient of silicon). The minority carriers generated by the illumination are collected by the electric field due to the surface band bending, and the resulting surface photovoltage is capacitively detected by a lock-in technique. The light intensity is varied in such a manner that for the different wavelengths, a constant surface photovoltage is obtained. In this case a plot of the light intensity versus the penetration depth α^{-1} yields a straight line with the diffusion length L as the intercept with the α^{-1} axis.

Our measurement system is fully automated, and wafers up to 6 in. in diameter can be investigated. The measured area on a wafer can be varied between about 1×1 and $5 \times 5\text{ cm}^2$; depending on the signal strength, typical measurement times are about 1–2 min.

For the present measurements wavelengths between 850

and 1020 nm were used which correspond to penetration depths of about 20–200 μm . We used data from Nartowitz and Goodman¹⁵ instead of ASTM values for the absorption coefficient α of silicon which results in approximately 10% larger diffusion lengths. The light intensity was usually in the range of several 10^{11} to some 10^{12} photons/($\text{cm}^2 \text{ s}$); therefore, by this method the *low-level* recombination lifetime is actually measured.

All measurements were carried out on B-doped Czochralski (Cz) and floating-zone (FZ) wafers (3–6 in. in diameter). The boron concentration of the investigated samples covered a range of about 10^{14} – 10^{16} cm^{-3} , but mostly samples with $1\text{--}3 \times 10^{15} \text{ cm}^{-3}$ were used. There was no preparation of the samples except an HF dip just before the measurement.

III. PRINCIPLE OF THE METHOD

A. The FeB pair reaction

The principle of the method hinges on the fact that iron in bulk Si is dissolved on an interstitial site (Fe_i)¹⁶ and that it is mobile at room temperature ($D \approx 10^{-15} \text{ cm}^2/\text{s}$). Positively charged Fe_i^+ can form immobile FeB pairs with negatively charged boron acceptor atoms B^- and other shallow acceptors like Al or Ga. Since both Fe_i and FeB introduce deep levels in the lower half of the silicon band gap,¹⁷ they can be detected by DLTS (Fig. 1). Fe_i is a deep donor with an energy level at about $E_v + 0.4 \text{ eV}$; the FeB pair forms a rather shallow donor level at $E_v + 0.1 \text{ eV}$.

The equilibrium of the point-defect reaction



depends on the temperature and the boron concentration. Figure 2 shows the interstitial fraction of the total Fe content as a function of temperature with the boron concentration as a parameter. The curves were calculated after an experimentally determined formula given by Lemke.¹⁸ At room temperature and $[\text{B}] > 10^{14} \text{ cm}^{-3}$, all Fe is bound in FeB pairs

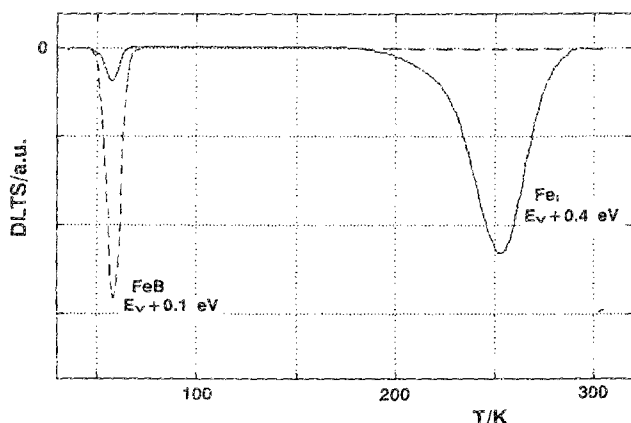


FIG. 1. DLTS spectrum of interstitial iron Fe_i and iron boron pairs FeB (rate window = 200 s^{-1}). The dissociation and pairing reaction (1) can be followed by the change in the amplitudes of the respective DLTS lines. Dashed curve: after storage at room temperature; solid curve: after annealing at 210°C for 3 min.

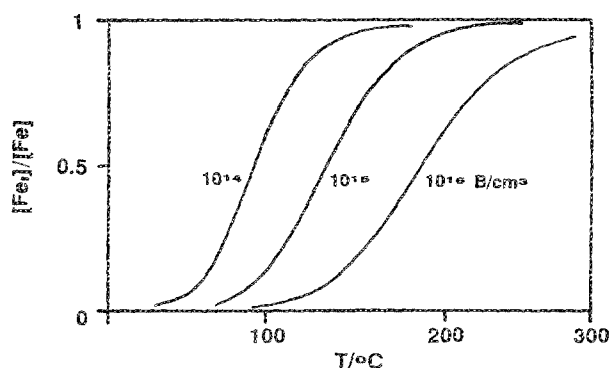


FIG. 2. Interstitial fraction of total dissolved iron content $[\text{Fe}_i]/[\text{Fe}] = [\text{Fe}_i]/([\text{Fe}_i] + [\text{FeB}])$ as a function of temperature T and boron concentration $[\text{B}]$ as a parameter (after Ref. 18).

in equilibrium, whereas at temperatures above approximately 200°C and $[\text{B}] < 10^{16} \text{ cm}^{-3}$, most Fe is on interstitial sites.

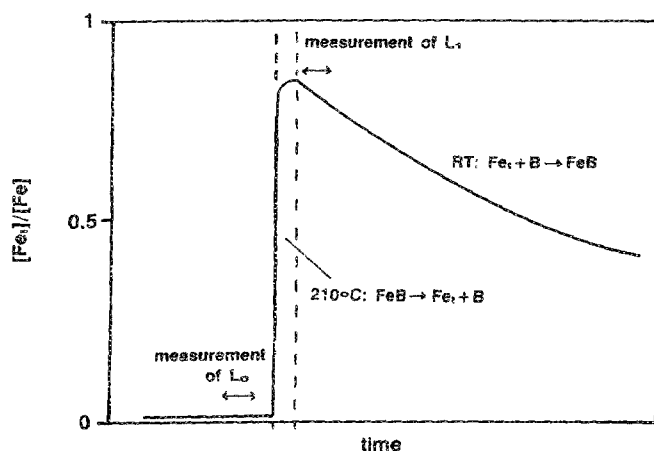
B. Modulation of the diffusion length L by FeB pairing

The essential idea of the Fe detection by measuring the diffusion length L is the fact that Fe_i with its comparatively deep level is more effective as a recombination center (see below) than FeB with a level close to the valence-band edge. Therefore, the pairing reaction (1) should affect the diffusion length of a given material. The experimental procedure to demonstrate this is illustrated in Fig. 3(a) which shows the interstitial Fe concentration during the measurement sequence. At first the diffusion length L_0 of a wafer with a Fe content of $1.1 \times 10^{13} \text{ cm}^{-3}$ was measured with all Fe bound in FeB pairs. Then the wafer was annealed at 210°C for 3 min and cooled quickly to room temperature by placing it onto an Al plate. By this heat treatment, reaction (1) is driven to the left; i.e., the FeB pairs are dissociated and interstitial Fe_i is formed [Figs. 1 and 3(a)]. After the anneal treatment the diffusion length (L_1) was measured again. As expected, the diffusion length changed from about 90 to $30 \mu\text{m}$ after the anneal treatment [Fig. 3(b)].

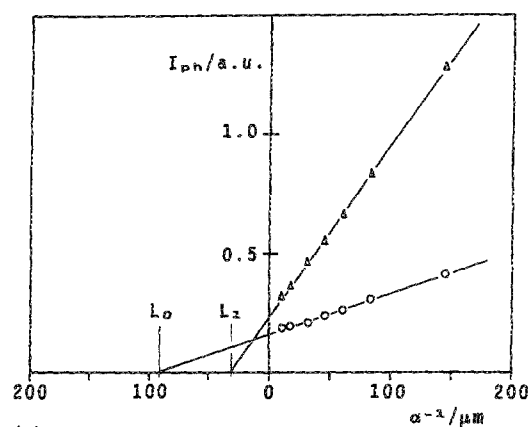
As shown below from the change in the diffusion length, the Fe concentration can be determined. The advantages of the SPV method compared to DLTS for measuring the Fe content in B-doped silicon are (i) virtually no preparation is required (except for an HF dip to remove an SiO_2 layer); the measurement requires only some minutes (rather than hours for DLTS with sample preparation); (ii) a large area (up to $5 \times 5 \text{ cm}^2$) can be sampled (Fig. 4); (iii) a wafer is sampled to a depth of about $100\text{--}200 \mu\text{m}$, compared to several μm for DLTS.

IV. DETERMINATION OF THE Fe CONCENTRATION BY SPV-DIFFUSION LENGTH MEASUREMENTS

In order to be able to relate the Fe concentration reliably to the decrease of the diffusion length caused by the FeB dissociation reaction, a number of conditions have to be fulfilled. The experiments described in this section have been designed to establish that these conditions are indeed met.



(a)



(b)

FIG. 3. (a) Schematic representation of the experimental procedure to determine the Fe concentration by diffusion length measurements. (b) Typical SPV measurements of the minority-carrier diffusion length of a Si wafer with an Fe content of $1.1 \times 10^{13} \text{ cm}^{-3}$ (DLTS result). ○: after long storage at room temperature (FeB dominant); Δ: after 3 min/210°C annealing (Fe_i dominant).

A. Reversibility of the pairing reaction/absence of precipitation

According to Fig. 2, more than 90% of the dissolved Fe is dissociated for temperatures above 200 °C and $[B] \approx 10^{15} \text{ cm}^{-3}$. It has been checked that equilibrium is reached within less than a minute by varying the time for the 210 °C an-

neal between 30 s and 1 h. Therefore, after 3 min the dissociation reaction



is essentially completed. However, it is conceivable that at about 200 °C, part of the mobile interstitial Fe atoms escape electrical detection by precipitation during the dissociation anneal. Therefore, the dissociation and pairing reaction was carried out many times for dissociation temperatures up to 250 °C.

It was ascertained both by SPV and DLTS measurements that reaction (1) is completely reversible at least up to 250 °C and annealing times up to 1 h. In fact, depending on the vendor and crystal type (FZ or Cz), an annealing temperature between 400 and 700 °C was required to induce Fe precipitation at all for Fe concentrations of the order of 10^{13} cm^{-3} and annealing times up to 1 h.

Therefore, the dissociation anneal at 210 °C for 3 min which is an essential part of our measuring procedure does not lead to a loss of interstitial iron by precipitation.

B. Pairing reaction during cooldown from 210 °C

A further potential source of error in the determination of the Fe concentration by SPV measurements is the back reaction



during cooldown from 210 °C, since in the temperature range 100–150 °C more than 50% of the Fe should be in pairs in thermal equilibrium (for $[B] \approx 10^{15} \text{ cm}^{-3}$) and the pairing reaction can take place within minutes. To test whether the back reaction can be controlled, different quenching methods from the anneal temperature were investigated. According DLTS and SPV measurements on specimens with Fe concentrations varying from 5×10^{11} to 10^{14} cm^{-3} , cooling in water, on an Al plate and in air, resulted in different fractions of interstitial iron after quenching to room temperature (Table I). Only quenching in water is fast enough to hold all Fe_i on interstitial sites; i.e., the equilibrium concentration of Fe_i at the anneal temperature can be frozen in, whereas only about 80% of Fe_i is left after cooling on an Al plate.

Although it would thus be best to cool in water, cooling on an Al block is a much more suitable method for routine measurements and has thus been adopted. The 20% loss of Fe_i by the pairing reaction is accounted for in the calibration.

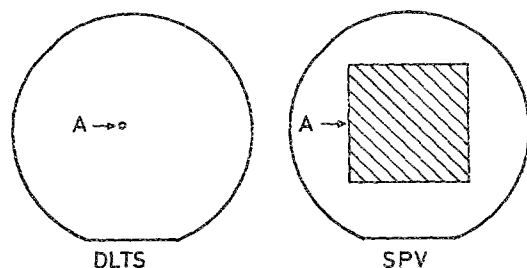


FIG. 4. Comparison of typical areas A on a 4-in. wafer sampled by DLTS and the SPV method. Also note that DLTS samples only a depth of some μm , whereas SPV detects defects that act as recombination centers to a depth of 100–200 μm .

TABLE I. Influence of the cooling rate after the dissociation anneal on the interstitial Fe concentration observed at room temperature. f^* denotes the fraction of the equilibrium concentration of Fe_i at the anneal temperature that can be frozen in.

Quenching method	Cooling rate	f^*
water	fast	1
Al-plate	medium	0.8
air	slow	0.5

C. Determination of a Fe surface contamination by SPV

As shown in Secs. IV A and IV B, the reaction (1) can be carried out in a well-controlled manner so as to measure the concentration of Fe dissolved in the bulk of the crystal. However, in practice, the *surface contamination* by Fe is as important if not more important. Therefore, it was investigated whether a surface Fe contamination can be transformed into a bulk contamination by a 1200 °C/30 s rapid anneal step.

To this end, a specimen with a homogeneous intentional surface contamination was subjected to a 1200 °C/30 s drive-in step in a nitrogen ambient with about 1% of oxygen by rapid thermal annealing (RTA). The in-depth Fe-diffusion profile was recorded by successive removal of thin layers by etching, deposition of a Schottky barrier, and determination of the Fe concentration by DLTS. The Fe concentration turns out to be homogeneous within about 20% (Fig. 5), at least for Fe concentrations well below the solubility limit of $2 \times 10^{16} \text{ cm}^{-3}$. We have indications that for $[\text{Fe}] > 10^{14} \text{ cm}^{-3}$, outdiffusion during cooldown can lead to inverted U-shaped Fe-concentration profiles.

Comparison of the Fe-surface concentration values before drive-in by total-reflection x-ray fluorescence (TXRF) analysis¹⁹ and the bulk values after drive-in showed that about 80% of the Fe on the surface ends up in the bulk; the rest presumably evaporates or is in near-surface Fe silicides.

In consequence, the SPV method can also be used to monitor a Fe surface contamination, if combined with a RTA drive-in step.

V. CALIBRATION

It is straightforward to show (Appendix A) that the decrease of the diffusion length after the dissociation anneal is related to the Fe concentration of the sample by

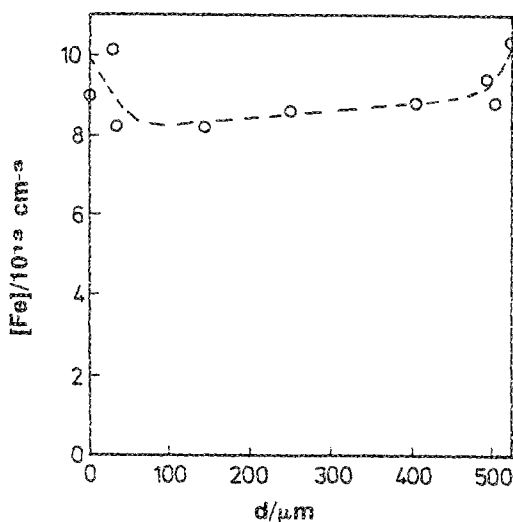


FIG. 5. Concentration profile of electrically active Fe after a 1200 °C/30 s drive-in step to diffuse an intentional homogeneous Fe surface contamination on both sides into the bulk of a 4-in. FZ wafer. The Fe concentration was determined by successive removal of layers and DLTS measurements on Schottky barriers.

$$[\text{Fe}] = \frac{D_n}{f} \left(\frac{1}{L_1^2} - \frac{1}{L_0^2} \right) / \left(C_n(\text{Fe}_i) - \frac{C_n(\text{FeB})}{\exp[(E_F - 0.1 \text{ eV})/k_B T]} \right). \quad (4)$$

$D_n = 37 \text{ cm}^2/\text{s}$ denotes the electron diffusion coefficient at room temperature, L_0 and L_1 are the measured diffusion lengths before and after annealing. f is a factor that compensates for the incomplete transformation to Fe_i . $C_n(\text{Fe}_i)$ and $C_n(\text{FeB})$ are the electron capture coefficients of Fe_i and FeB , respectively.

Note that this relation also holds if there are other recombination centers in the sample, for instance, oxygen precipitates or other metallic impurities. For Eq. (4) to hold, it is, however, necessary that Fe_i is the *only electrically active impurity to undergo a point-defect reaction at 210 °C*, which in our experience is true for most practical cases.

In equilibrium at 210 °C, approximately 90% of the total Fe is as Fe_i for $[\text{B}] = 1\text{--}3 \times 10^{15} \text{ cm}^{-3}$. Since only about 80% of the Fe_i can be frozen in by cooling the wafer on an Al plate (see Sec. IV B), we have $f \approx 0.7$ for our experimental conditions.

The unknown electron-capture coefficients of Fe_i and FeB were determined by combined SPV and DLTS measurements on a number of Cz and FZ wafers after intentional contamination with different Fe concentrations. To this end as-received wafers were contaminated in a controlled manner by immersing them in a chemical solution containing different amounts of Fe. With TXRF no other impurities besides Fe were detected on the wafer surface (detection limit $\approx 10^{11} \text{ cm}^{-2}$) after the contamination process. A RTA drive-in step (1200 °C/30 s) was used to transform the Fe surface contamination into a bulk contamination (see Sec. IV C). Prior to the drive-in step, the diffusion length of the samples was larger than 300 μm, and no electrically active defects were found by DLTS measurements (detection limit = 10^{11} cm^{-3}) using both majority- and minority-carrier excitation (minority carriers were created by optical excitation with $\lambda = 890 \text{ nm}$). After RTA only the well-known levels due to Fe (see Fig. 1) were revealed by DLTS.

For the determination of the electron-capture coefficients, the following procedures have been adopted: (i) measurement of the diffusion length L_0 (at steady state at room temperature more than 99% of the dissolved Fe is in FeB pairs), (ii) 210 °C/3 min anneal and quench to room temperature on an Al plate (about 70% of the dissolved Fe as Fe_i), and (iii) measurement of the diffusion length L_1 . After the diffusion length measurements, the total Fe concentration was determined on the same wafers by DLTS. In Fig. 6 the result is plotted as L^2 vs $[\text{Fe}]$. Since according to DLTS the wafers contained only Fe as electrically active impurities, the expected dependence of $L^2 \propto 1/[\text{Fe}]$ [see Eqs. (A1), (A3a), and (A3b)] is fulfilled both for L_0 and L_1 .

A fit of Eqs. (A4) and (A5) to the data (with $\tau_R \rightarrow \infty$) yields

$$C_n(\text{FeB})/\exp[(E_F - 0.1 \text{ eV})/k_B T] = 5 \times 10^{-8} \text{ cm}^3/\text{s},$$

$$C_n(\text{Fe}_i) = 5.5 \times 10^{-7} \text{ cm}^3/\text{s},$$

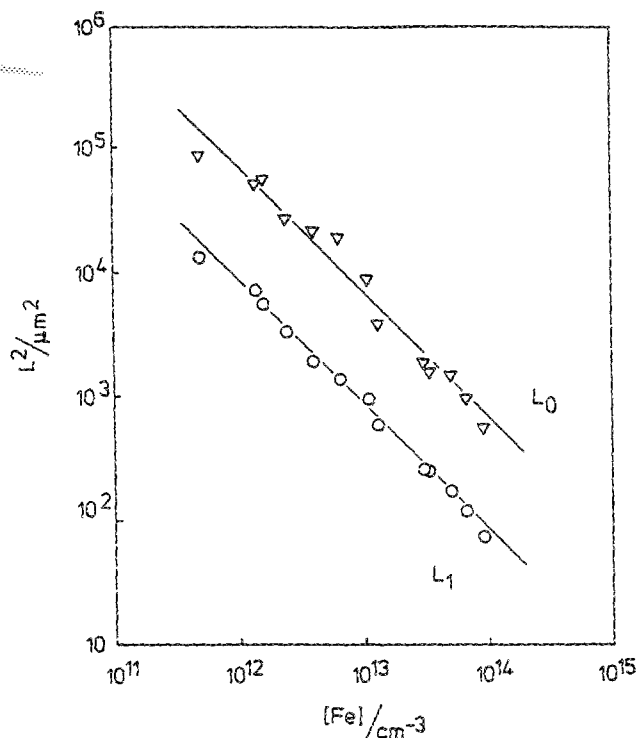


FIG. 6. DLTS calibration data for the SPV method. The Fe concentration was measured on homogeneously contaminated wafers by DLTS; the diffusion lengths L_0 and L_1 were measured before (∇) and after (\circ) a dissociation anneal at 210 °C. In all cases only Fe was detected by DLTS.

i.e., in SPV measurements Fe_i acts as a 10 times more effective recombination center than FeB. The factor of 10 in the recombination efficiency means that there is a factor of ≈ 3 between the respective diffusion lengths L_0 and L_1 .

Inserting all numerical values into Eq. (4), the following formula for the calculation of the Fe concentration is obtained:

$$[\text{Fe}]/\text{cm}^{-3} = 1.06 \times 10^{16} (1/L_1^2 - 1/L_0^2), \quad (5)$$

where the values of L have to be inserted in μm .

The data presented in Fig. 6 allow for an estimation of the sensitivity of the method. Since $L^2 \propto 1/[\text{Fe}]$ is fulfilled even for $[\text{Fe}] < 10^{12} \text{ cm}^{-3}$, it is surely better than 10^{12} cm^{-3} . To our experience about $2\text{--}5 \times 10^{11} \text{ cm}^{-3}$ can be reliably detected if Fe is the dominant recombination center. For this case the accuracy of the method is $\approx 20\%$. If other electrically active defects are present, the sensitivity for Fe detection depends on the accuracy of the diffusion length measurement which is about $\pm 10\%$ for our system.

VI. "FINGERPRINTS" OF Fe IN THE SPV METHOD

The results of the previous sections show that the Fe concentration can be determined by SPV provided no other point defect reactions take place at 210 °C. In this section we show that the SPV method can also give quite good positive proof as to whether Fe is indeed the major electrically active impurity and provide a "fingerprint" which for all intents and purposes can be regarded as a way to identify Fe without

having to resort to DLTS or another more involved detection method.

A. Ratio of diffusion lengths

The factor of 10 in the recombination efficiency of FeB and Fe_i, i.e., a factor of ≈ 3 in the diffusion lengths L_0 and L_1 , can be regarded as a kind of hallmark of the FeB point defect reaction, since the probability of another point-defect reaction with a threshold of about 200 °C or below with this characteristic factor in the respective recombination efficiency is quite low.

It has been our experience from many hundreds of measurements that $L_0/L_1 \approx 3$ is fulfilled rather well for material with $[\text{B}] \approx 10^{15} \text{ cm}^{-3}$.

According to the Shockley-Read theory,²⁰ the recombination efficiency of FeB should depend on the boron concentration of the sample (see Appendix A) with a decrease of L_0/L_1 for increasing $[\text{B}]$. We have observed indeed such a dependence during our investigations. We found $L_0/L_1 \approx 2$ as typical for $[\text{B}] \approx 10^{16} \text{ cm}^{-3}$ and $L_0/L_1 \approx 4$ for $[\text{B}] < 5 \times 10^{14} \text{ cm}^{-3}$. In any case, strong deviations from this characteristic values for L_0/L_1 indicate the presence of other recombination centers or an extremely inhomogeneous lateral distribution of Fe.

B. Pairing kinetics

A further but more time-consuming way to identify Fe by SPV measurements is to measure the diffusion coefficient of interstitial iron at room temperature by monitoring the pairing kinetics [Eq. (3)]. This can be simply done by measuring the diffusion length as a function of time after the 210 °C dissociation anneal. Figure 7 shows the normalized concentration of interstitial iron, c_{Fe_i} , as a function of time calculated by Eq. (4) from the diffusion lengths. As expected for a pairing reaction, first-order kinetics is observed. The

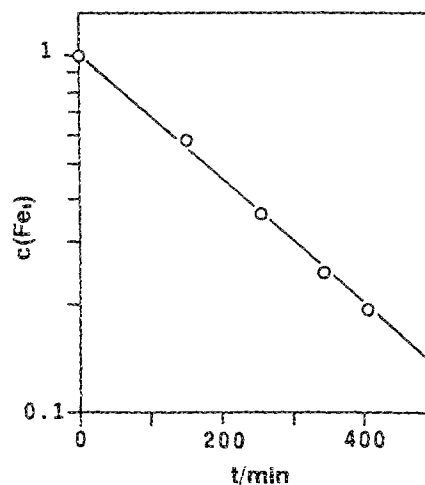


FIG. 7. Decrease of the normalized interstitial iron concentration $c_{\text{Fe}_i} = [\text{Fe}_i]/[\text{Fe}_i](t=0)$ after annealing at 210 °C due to the FeB pairing reaction at room temperature.

time constant τ for the formation of FeB pairs depends on the boron concentration $[B]$ and on the diffusion coefficient of interstitial Fe, and is given by (formula from Ref. 21, diffusion data from Ref. 16)

$$\tau = 4.3 \times 10^5 T / [B] \exp(0.68 \text{ eV} / k_B T). \quad (6)$$

To ascertain whether the measurement of τ can be used as a further fingerprint for Fe, the time constant was determined for a $[B]$ range from 10^{14} to 10^{16} cm^{-3} . The expected $1/[B]$ dependence of τ is fulfilled in an excellent manner (Fig. 8).

Therefore, SPV measurements can also serve to identify Fe to a reasonable degree of certainty without having to go back to DLTS measurements.

VII. APPLICATIONS AND EXAMPLES

In the following we report on two examples which have been chosen to demonstrate both the practical usefulness of the method and serve to further elucidate the method itself.

A. Fe contamination of as-received wafers

The *bulk* of Si crystals can be contaminated by Fe during crystal growth, whereas wafer shaping and cleaning operations are prone to cause Fe contamination of the wafer surface.

Inspection of a large number of incoming wafers from several manufacturers (Fig. 9) has shown that the concentration of dissolved Fe in the bulk is usually less than $5 \times 10^{11} \text{ cm}^{-3}$. Only in few cases could Fe be detected in incoming wafers with concentrations up to several 10^{12} cm^{-3} .

By contrast, a noticeable contamination of the wafer surface as detected by a $1200^\circ\text{C}/30 \text{ s}$ drive-in step and subsequent SPV measurements seems to be the rule rather than the exception. Volume concentrations of Fe between $\approx 10^{12}$ and 10^{13} cm^{-3} are typical, but in rare cases also values around $5 \times 10^{11} \text{ cm}^{-3}$ can be found. The Fe concentrations

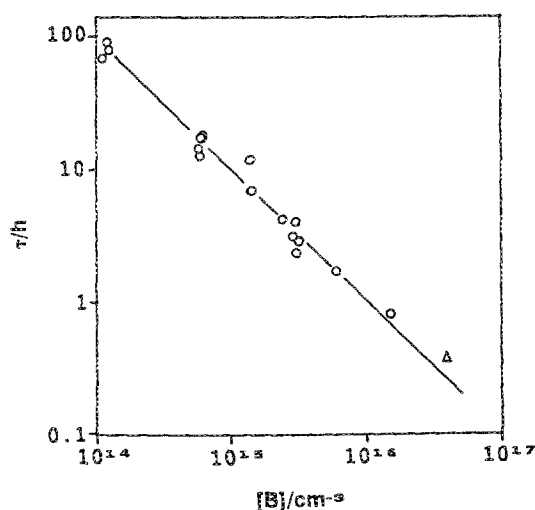


FIG. 8. Time constant τ of the FeB pairing reaction at $298 \pm 3 \text{ K}$ as a function of the boron concentration $[B]$. (O: data points by SPV; Δ : DLTS result from Hansen.²³ The solid line has been calculated after Eq. (6) for a temperature of 298 K .

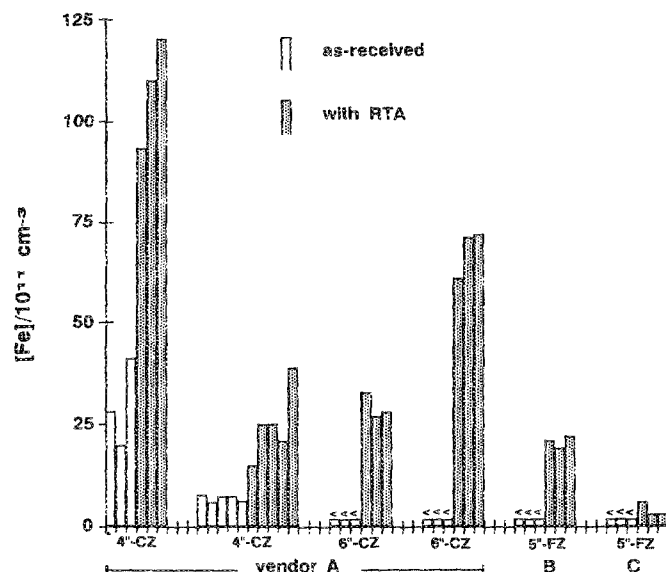


FIG. 9. Histogram of Fe contents determined by the SPV method for different Cz and FZ wafer lots of several vendors before (as-received) and after rapid thermal annealing (RTA) at $1200^\circ\text{C}/30 \text{ s}$.

measured after the RTA drive-in step correspond to a typical surface contamination level of about $0.25\text{--}2.5 \times 10^{11} \text{ cm}^{-2}$ for incoming wafers.

B. Inhomogeneous contamination of wafers

An unintentional contamination of a wafer is, as a rule, not homogeneous. An example for this is given in the upper part of Fig. 10, which shows a haze picture of a 4-in. wafer after Secco defect etching. The contamination with haze-forming impurities—to our experience Ni and Cu in most

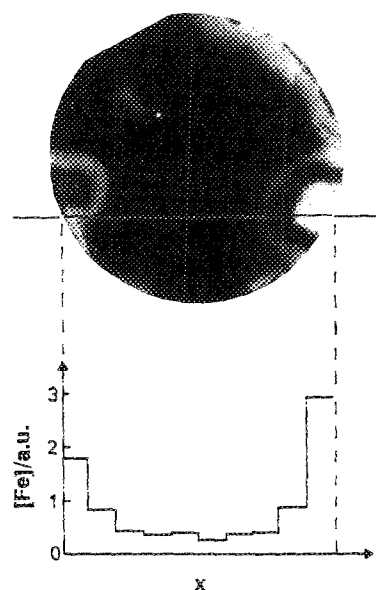


FIG. 10. Fe profile across an inhomogeneously contaminated 4-in. wafer. In the upper figure a haze picture of the wafer after Secco defect etching is shown. Highly contaminated regions look bright due to a high density of surface near precipitates. The lower figure shows the Fe profile along the indicated line as determined by the SPV method.

cases—is low in the middle of the wafer (dark regions) and high in the bright areas at the edge.

SPV measurements were performed along the indicated line with a spatial resolution of ≈ 1 cm and a total measurement time of about 30 min. The result of this measurement is depicted in the lower part of the figure. The good correspondence between Fe concentration and the haze strength points to stainless steel (with Ni as the haze-forming element) as the contamination source in this case.

This example demonstrates that SPV can yield a wafer map with moderate spatial resolution at the expense of a longer measuring time. This point is especially valuable because the haze method has become rather unreliable for delineating Fe distributions.¹⁰

VIII. SUMMARY AND CONCLUSION

It has been shown that the surface photovoltage method to determine the minority-carrier diffusion length is suitable to detect Fe in boron doped silicon ($[B]$ between 10^{14} and some 10^{16} cm⁻³). The technique has a sensitivity of some 10^{11} cm⁻³ and an accuracy of about 20%, if Fe is the dominant recombination center. Since the method is fast (several minutes), can sample large areas (up to 25 cm²), and is practically preparation free, it is suitable for contamination-monitoring purposes.

The Fe concentration is determined by the modulation of the minority-carrier diffusion length L by the reversible point-defect reaction



Interstitial iron Fe_i is about 10 times more effective as a recombination center than FeB by low-level lifetime measurements and therefore reduces the minority-carrier diffusion length more strongly.

It has been shown that the point-defect reaction can be controlled sufficiently well by a dissociation anneal at 210 °C for 3 min for a quantitative determination of the Fe content, provided Fe is the only recombination active impurity to undergo a point-defect reaction at this temperature. If Fe is the dominating recombination center, a factor of 3 in the modulation of the diffusion length (for $[B] \approx 10^{15}$ cm⁻³) and the time constant for the pairing reaction can serve to identify Fe.

It is conceivable that the principle for the Fe detection can also be applied to contactless lifetime and diffusion length measurements which are becoming more and more popular as in-line contamination control techniques,²² provided a reliable calibration can be obtained for such measurements.

ACKNOWLEDGMENTS

The authors are indebted to G. Götz, B. Göttinger, and G. Asam for assistance with the experimental work. This work was supported by the Federal Department of Science and Technology (NT 2696).

APPENDIX A: CALCULATION OF THE Fe CONCENTRATION FROM THE MODULATION OF THE DIFFUSION LENGTH

The diffusion length L and lifetime τ of the minority carriers in a p -type semiconductor are connected by the following equation:

$$L^2 = D_n \tau, \quad (\text{A1})$$

with $D_n = 37$ cm²/s being the electron diffusion coefficient at room temperature. If the semiconductor contains several different electrically active impurities i , each impurity contributes to the lifetime τ . For this case the resulting lifetime is given by

$$1/\tau = \sum 1/\tau_i. \quad (\text{A2})$$

According to the Shockley–Read recombination model,²⁰ the τ_i are determined by the concentration, the energy level, and the carrier-capture coefficients of the impurities. For low injection of excess carriers during the measurement, which is the case for the SPV method (see Sec. II), the lifetime is totally controlled by the lifetime of the minority carriers. The following expressions are obtained for interstitial Fe_i and FeB pairs in p -type silicon:

$$\tau_{\text{FeB}} = \exp[(E_F - 0.1 \text{ eV})/k_B T] / \{C_n(\text{FeB})[\text{FeB}]\}, \quad (\text{A3a})$$

$$\tau_{\text{Fe}_i} = 1/\{C_n(\text{Fe}_i)[\text{Fe}_i]\}. \quad (\text{A3b})$$

$C_n(\text{FeB})$ and $C_n(\text{Fe}_i)$ are the electron-capture coefficients of FeB pairs and interstitial Fe_i , respectively. Since the energy level of FeB ($E_F + 0.1$ eV) is rather shallow, its influence on the lifetime is reduced by $\exp[(E_F - 0.1 \text{ eV})/k_B T]$, where E_F is the Fermi level of the sample. For a boron concentration of about 10^{15} cm⁻³ and room temperature, the exponential term in Eq. (A3a) is of the order of 100. As will be shown below, this term is the main reason that FeB has much less influence on the low-level lifetime than interstitial Fe_i .

Let us now consider a sample with a total Fe concentration of $[\text{Fe}] = [\text{Fe}_i] + [\text{FeB}]$. At room temperature in steady state, all Fe is bound in FeB pairs, which means $[\text{FeB}] = [\text{Fe}]$. This is fulfilled for all samples with $[B] > 10^{14}$ cm⁻³ (see Fig. 2). With Eqs. (A2) and (A3a), the lifetime can be expressed as

$$1/\tau_0 = 1/\tau_R + C_n(\text{FeB})[\text{Fe}] / \exp[(E_F - 0.1 \text{ eV})/k_B T]. \quad (\text{A4})$$

In this equation τ_R takes into account the influence of all other additional impurities on the lifetime, e.g., other metals or oxygen precipitates.

After a short annealing above 200 °C and quenching to room temperature, a fraction $f = [\text{Fe}_i]/[\text{Fe}]$ is on interstitial sites and $1 - f$ is still bound in FeB pairs. Under the assumption that the contribution of all other impurities does not change during the anneal treatment, which to our experience is true in most cases, the lifetime is given by

$$1/\tau_1 = 1/\tau_R + (1 - f)C_n(\text{FeB})[\text{Fe}] / \exp[(E_F - 0.1 \text{ eV})/k_B T] + fC_n(\text{Fe}_i)[\text{Fe}]. \quad (\text{A5})$$

By forming the difference between Eqs. (A4) and (A5), the contribution of Fe to the lifetime is separated. With Eq. (A1) and solving for [Fe], it finally follows

$$[\text{Fe}] = \frac{D_n}{f} \left(\frac{1}{L_1^2} - \frac{1}{L_0^2} \right) / \left(C_n(\text{Fe}_i) - \frac{C_n(\text{FeB})}{\exp[(E_F - 0.1 \text{ eV})/k_B T]} \right). \quad (\text{A6})$$

f , the part of Fe on interstitial sites after the annealing step, is determined by the equilibrium concentration of Fe, at the annealing temperature and by the FeB pair formation during cooldown to room temperature. The equilibrium concentration of Fe_i is approximately 0.9 [Fe] at anneal temperatures in the range of 200–250 °C and [B] around 10^{15} cm^{-3} (see Fig. 2). After quenching the samples to room temperature on an Al plate, about 80% of the equilibrium concentration of Fe_i at the anneal temperature remain on interstitial sites (see Sec. III B). Therefore, we have

$$f \approx 0.7,$$

for the experimental conditions of this study.

The electron-capture coefficients of Fe_i and FeB were determined by combined SPV/DLTS measurements described in Sec. IV. The following values were obtained:

$$C_n(\text{FeB})/\exp[(E_F - 0.1 \text{ eV})/k_B T] = 5 \times 10^{-8} \text{ cm}^3/\text{s},$$

$$C_n(\text{Fe}_i) = 5.5 \times 10^{-7} \text{ cm}^3/\text{s}.$$

Since $\exp[(E_F - 0.1 \text{ eV})/k_B T] \approx 100$ for our samples, it follows that the electron-capture coefficient of FeB is about

$$C_n(\text{FeB}) \approx 5 \times 10^{-6} \text{ cm}^3/\text{s},$$

i.e., from this, FeB should be a 10 times stronger recombination center than Fe_i . Therefore, the rather shallow energy level of FeB is actually the reason for the fact that interstitial Fe appears as the stronger recombination center in *low-level* lifetime measurements.

For *high-level* lifetime measurements, both the lifetime of minority and majority carriers contribute to the measured lifetime. Estimations according to Shockley–Read theory with published values for the hole capture coefficients of FeB and Fe_i (Ref. 17) show that in this case the recombination behavior should be reversed; i.e., FeB should reduce the high-level lifetime more than Fe_i . This result is in agreement with observations described in the literature¹⁸ which indicate, indeed, a decrease of the high-level lifetime for an increase of the FeB concentration.

- ¹ B. O. Kolbesen and H. P. Strunk, *VLSI Electron. Microstruct. Sci.* **12**, 143 (1985).
- ² H. R. Huff and F. Shimura, *Solid State Technol.* **28**, 103 (1985).
- ³ B. T. Murphy, *Proc. IEEE* **52**, 1537 (1964).
- ⁴ K. Honda, A. Ohsawa, and N. Toyokura, *J. Appl. Phys.* **62**, 1960 (1987).
- ⁵ A. G. Cullis and L. E. Katz, *Philos. Mag.* **30**, 1419 (1974).
- ⁶ P. Augustus, *Semicond. Int.* **1985**, 88 (Nov. 1985).
- ⁷ P. J. Ward, *J. Electrochem. Soc.* **129**, 2573 (1982).
- ⁸ B. O. Kolbesen and W. Pamler, *Fresenius Z. Anal. Chem.* **333**, 561 (1989).
- ⁹ K. Graff, in *Aggregation Phenomena of Point Defects in Silicon*, edited by E. Sirtl, J. Goorissen, and P. Wagner (Electrochemical Society, Pennington, NJ, 1983), p. 121.
- ¹⁰ K. Graff (private communication, 1988).
- ¹¹ *Lifetime Factors in Silicon*, ASTM STP 712 (American Society for Testing and Materials, Philadelphia, PA, 1979).
- ¹² G. Zoth and W. Bergholz, *J. Electrochem. Soc. Ext. Abstr.* **88-1**, 273 (1988).
- ¹³ A. M. Goodman, *J. Appl. Phys.* **32**, 2550 (1961).
- ¹⁴ ASTM Report F391-78, 1979 Annual Book of ASTM Standards, Philadelphia, 1979.
- ¹⁵ E. S. Nartowitz and A. M. Goodman, *J. Electrochem. Soc.* **132**, 2992 (1985).
- ¹⁶ E. R. Weber, *Appl. Phys. A* **30**, 1 (1983).
- ¹⁷ K. Graff and H. Pieper, in *Semiconductor Silicon 1981*, edited by H. R. Huff, R. J. Kriegler, and Y. Takeishi (Electrochemical Society, Pennington, NJ, 1981), p. 331.
- ¹⁸ H. Lemke, *Phys. Status Solidi A* **64**, 215 (1981).
- ¹⁹ V. Penka and W. Hub, *Spectrochim. Acta* **44B**, 483 (1989).
- ²⁰ W. Shockley and W. T. Read, Jr., *Phys. Rev.* **87**, 835 (1952).
- ²¹ H. Reiss, C. S. Fuller, and F. J. Morin, *Bell. Syst. Tech. J.* **35**, 535 (1956).
- ²² M. Fung, *J. Electrochem. Soc. Ext. Abstr.* **88-1**, 269 (1988).
- ²³ J. Hansen (private communication, 1987).